Rotational Coherence Spectroscopy and Structure of Naphthalene Trimer

Peyman Benharash, Michael J. Gleason, and Peter M. Felker

Department of Chemistry and Biochemistry, University of California, Los Angeles, California 90095-1569

Received: December 4, 1998; In Final Form: February 2, 1999

We present the results of rotational coherence spectroscopy (RCS) experiments on jet-cooled naphthalene trimer. The RCS results, obtained by mass-selective, time-resolved ionization depletion, indicate that the species is an oblate symmetric top with rotational constants $B = 167 \pm 1$ MHz and $C = 141 \pm 1$ MHz. These constants are consistent with a cluster in which the long axes of three cyclically-arranged, symmetrically equivalent naphthalene moieties are parallel to one another and to the symmetry axis of the cluster. The distances between the centers of mass of the moieties in this structure are determined to be 4.925 ± 0.020 Å from the rotational constants. The results are consistent with ab initio and empirical force-field calculations of the species' structure (see Gonzalez and Lim, preceding Letter) and with the results of prior vibrational and vibronic spectroscopic studies.

I. Introduction

The naphthalene trimer has been the subject of several recent studies.[1−12] One's interest in this species arises from the motivation to understand the intermolecular forces between aromatic molecules, as well as from the interesting activated excimer-formation dynamics that the cluster exhibits[3−7] upon excitation to its S_1 manifold. One of the properties of the species that has been of greatest interest is its geometry, given that it is central to understanding or predicting the other properties and given that knowledge of the geometry provides an important benchmark for the evaluation of any potential-energy surfaces put forth to describe its intermolecular bonding.

The current information on the geometry of naphthalene trimer arises from four sources. First, vibronic spectroscopy (i.e., mass-selective resonantly enhanced multiphoton ionization) pertaining to the $S_1 \leftarrow S_0$ bands of several isotopomers has indicated that the species has three symmetrically equivalent monomer moieties.[3,7,8] Second, nonlinear Raman spectroscopy (i.e., mass-selective, ionization-detected stimulated Raman spectroscopy) pertaining to monomer-localized vibrational excitations in the cluster strongly corroborate this interpretation.[8] Third, nonlinear Raman spectroscopy relating to intermolecular vibrational transitions in four trimer isotopomers and to the pendular band contours associated with those transitions provide compelling evidence that the cluster is such that the three symmetrically equivalent naphthalene moieties are arranged with their long axes parallel to one another and to the C_3 symmetry axis of the species.[8,9,11] Finally, the minimum-energy structure of the species calculated on a semi-empirical potential-energy surface is consistent with the aforementioned experimental results.[8,11,12]

While there appears to be a convergence of experimental and theoretical results as to the qualitative nature of naphthalene trimer's geometry, the additional structural information potentially available from rotational spectroscopy on the species could provide the final proof for that geometry. Moreover, quantitative structural details unavailable from vibrational and vibronic spectroscopic results could be extracted from high-resolution rotational results.

In this paper we report the measurement of the rotational constants of perprotonated naphthalene trimer by rotational coherence spectroscopy (RCS), as implemented by mass-selective, time-resolved ionization depletion[13] (TRID). The results are completely consistent with a C_{3h} species in which the naphthalene moieties have their long axes parallel. They also allow for the extraction of a monomer-to-monomer center-of-mass distance of 4.925 ± 0.020 Å in the cluster. Moreover, all of the geometrical details derived from the RCS measurements are consistent with the computational (i.e., *ab initio* and molecular mechanics) results recently obtained by Gonzalez and Lim.[10] Finally, the experiments clearly demonstrate that the sensitivity of ionization detection and the selectivity of mass analysis that are both available with RCS-TRID allow for the possibility of obtaining high-resolution structural results on clusters that would not be obtainable in any other way.

II. Experimental Section

RCS was implemented by mass-selective time-resolved ionization depletion.[13] TRID involves first preparing rotational coherences by a linearly polarized pump pulse that is resonant with a vibronic transition of the species of interest. Coherences in the rotational manifold of the ground vibronic state and in that of the excited vibronic state are both prepared with essentially equal amplitudes by this process. Second, a variably delayed, linearly polarized probe pulse at the same frequency samples the time evolution of these coherences. The effect of the probe pulse is to map such time evolution onto the population of the excited vibronic level. Finally, the excited-state population is converted into a photoion signal by a third laser pulse. Mass-selected photoions are detected as a function of pump-probe delay to yield a TRID trace. In this scheme the pump and probe pulses must be short enough to resolve the time evolution of rotational coherences in the species. Hence, pulses with widths on the scale of several to tens of picoseconds are required. The only constraint on the width of the photoionization pulse, however, is that it be sufficiently short to photoionize excited species effectively. Widths of nanoseconds or longer can be suitable, depending on the relevant excited-state lifetime.

10.1021/jp984636c CCC: $18.00
Published on Web 03/02/1999

The apparatus employed to implement mass-selective RCS-TRID was as follows. Pump and probe pulses were generated by frequency doubling the amplified output of a synchronously pumped dye laser. The home-built dye laser (DCM in ethylene glycol as dye) was pumped by the frequency-doubled pulse-train output (~80 MHz repetition rate, ~2 W average power, 60 ps pulsewidths) of an acousto-optically mode-locked Nd:YAG laser (Spectron SL903). The linearly-polarized pulse-train output of the dye laser (~0.15 W average power, 8 ps pulsewidths, 2 cm^{-1} bandwidth), which was tuned with a three-plate birefringent filter/fine-tuning etalon combination, was amplified by a home-built, three-stage dye amplifier. The dye amplifier was pumped by the frequency-doubled output of a Nd:YAG regenerative amplifier (Continuum RGA 69), seeded by the output of the Spectron Nd:YAG and operating at 20 Hz. The output of the dye amplifier consisted of a 20-Hz pulse train of polarized pulses having about the same frequency, bandwidth, and pulsewidth of the dye-laser output but with energies of about 2 mJ per pulse. The amplified pulse train was frequency-doubled in β-barium borate, and the resulting UV pulses were then split into pump and probe pulse trains by a 50/50 beam splitter. Each pulse train was reflected back to this same beam splitter by hollow corner-cube retroreflectors, the retroreflector for the pump pulses being stationary and that for the probe pulses being mounted on a stepper-motor-driven, computer-controlled linear translation stage (Velmex Unislide). After being combined collinearly on the beam splitter, the pump and probe pulse trains were then mildly focused into the skimmed molecular-beam sample in the ion-acceleration region of a time-of-flight mass spectrometer. The photoionization pulses were generated by frequency-doubling the output of a dye laser (Spectra Physics PDL-2) pumped by the 532-nm output of a nanosecond Nd:YAG laser (Spectra Physics DCR-2A). The timing of the photoionization pulses with respect to the pump and probe pulses was accomplished electronically by synchronizing the firing of the DCR-2A laser with that of the regenerative amplifier by the use of a delay generator (Stanford DG 535). Generally, the ~7-ns photoionization pulse was delayed by about 40 ns at the sample with respect to the probe pulse. The photoionization pulse train was very mildly focused into the molecular beam sample where it intersected the pump and probe fields collinearly but in a counter-propagating direction.

The molecular-beam apparatus employed was essentially identical to that described in other papers from this group.[8,9] Briefly, the seeded, pulsed molecular beam was generated by a solenoid-driven valve (General Valve Series 9), the orifice (0.1 cm in diam) through which a mixture of naphthalene vapor and helium (1 part in 1000 at 300 psig total pressure) expanded into vacuum. The molecular beam was skimmed by a conical skimmer (1 cm diameter orifice) at a distance of about 8 cm from the expansion source. The skimmed beam then entered the acceleration region of a differentially pumped time-of-flight mass spectrometer of Wiley−McClaren design. The molecular beam intersected the excitation fields in this region at a total distance of 20 cm from the expansion orifice. Photoions were accelerated in a direction perpendicular to both the molecular-beam and laser-field propagation directions and detected by a dual microchannel plate arrangement. The output of this detector was amplified and then averaged by a boxcar integrator. Data collection consisted of monitoring with a computer the output of the boxcar (with its gate set to detect photoions with mass 384 amu) as a function of the delay between pump and probe pulses.

The results presented below pertain to perprotonated naphthalene trimer excited by pump and probe pulses resonant with its vibronic transition at 32 374 cm^{-1}.[1−3,7,8] This vibronic band correlates with the $\bar{8}_0^1$ vibronic transition of naphthalene monomer,[14] which is polarized along the short in-plane axis of the molecule. The photoionization pulse was tuned to a frequency of 30 480 cm^{-1}, which is smaller than the frequency of the $S_1 \leftarrow S_0$ 0_0^0 band of the trimer but large enough to effect photoionization in a single-photon step from the S_1 manifold. Since TRID is a depletion spectroscopy, in which the signal consists of small transients on top of a large, unmodulated background, it is important to try to maximize the modulation depth of such transients. One of the ways that this was done in this study was to adjust excitation field intensities such that one-color photoion signals at 384 amu were only a small fraction of the two-color signal at that mass.

As mentioned above, the degenerate RCS-TRID scheme that we employ creates and probes both ground-state and excited-state rotational coherences.[13] As such, RCS transients dependent on ground-state rotational constants and ones dependent on excited-state constants can both appear in the same experimental trace. In the case of naphthalene trimer excited via its $\bar{8}_0^1$ band, however, S_1 transients may not contribute appreciably because of rapid intramolecular vibrational-energy redistribution out of the $\bar{8}^1$ level and into vibrationally relaxed S_1 states.[3] This process, even if it preserves the S_1 rotational coherences created by the pump pulse, may prevent effective probing of those coherences at the probe-pulse frequency. The upshot is that it is unclear whether the transients measured in the present experiments reflect just S_0 rotational constants or both S_0 and S_1 constants. In any case, one does not expect the differences between such constants to be so large as to make an appreciable difference in the conclusions set forth below.

III. Results and Discussion

Figure 1 (top) shows measured RCS-TRID results corresponding to excitation of the $\bar{8}_0^1$ band of perprotonated naphthalene trimer. The trace is a compilation of several individual scans taken over smaller delay ranges. Obvious in the experimental data are the four RCS transients labeled "J". These features are equally spaced from one another by 1500 ps. Hence, they are clearly of the same type. Further, their alternating polarity and their intensity pattern indicate them to be *J*-type transients[15] arising from a symmetric or near-symmetric top. This assignment and the transient positions dictate a value of 167 MHz for the $\bar{B}$ rotational constant of the trimer, where $\bar{B}$ is either the *B* constant of a symmetric top, $(A + B)/2$ of a near-oblate top, or $(B + C)/2$ of a near-prolate top.

Also present in the experimental trace of Figure 1, though less obvious than the *J*-type features, are transients in the vicinity of 1775 and 3450 ps (labeled "C"). Expanded views of these transients are shown in Figure 2. The positions of these two features clearly indicate that they are of the same type. Moreover, the strange shape of the one at 1775 ps indicates[15] that they are either *A*-type (appearing at delays equal to $n/4A$, $n = 1,2,...$) or *C*-type (appearing at $n/4C$). Since 1775 ps is greater than the delay associated with the first *J*-type feature (which occurs at $1/4\bar{B}$), the only possible assignment is *C*-type. Accordingly, one extracts a value of 141 MHz for the *C* constant of the trimer. Further, since *C*-type transients are prominent only when the transition dipole of the vibronic band being pumped has a large component along the principal axis having the smallest moment of inertia, it is clear that the $\bar{8}_0^1$ band of the trimer is polarized in such a fashion.

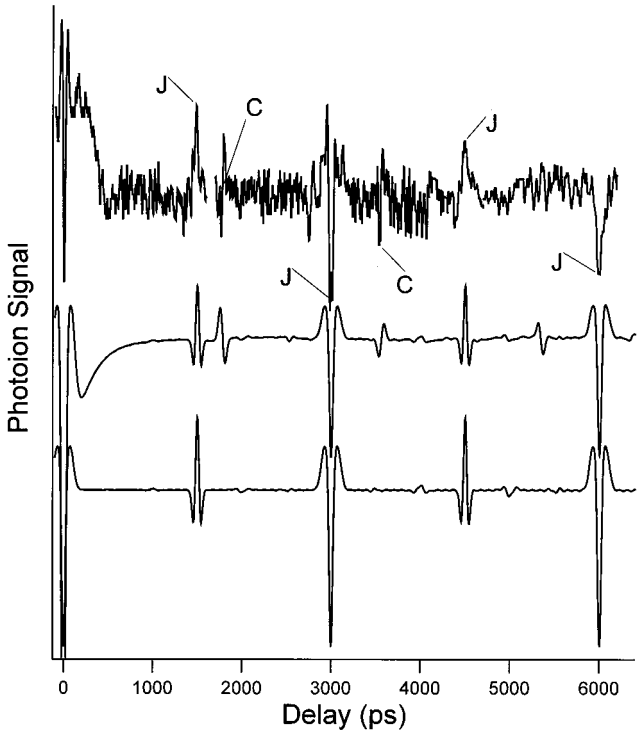

Figure 1. (Top) Measured RCS-TRID trace corresponding to excitation of the $\bar{8}_0^1$ band of perprotonated naphthalene trimer with parallel-polarized pump and probe pulses and detection of the parent-ion mass. (Middle) Simulated RCS trace obtained by assuming an oblate symmetric top with rotational constants $B = 167$ and $C = 141$ MHz, a perpendicular-type transition moment, a temperature of 1.5 K, and parallel-polarized pump and probe processes. (Bottom) Same as the middle but for a parallel-type transition moment.

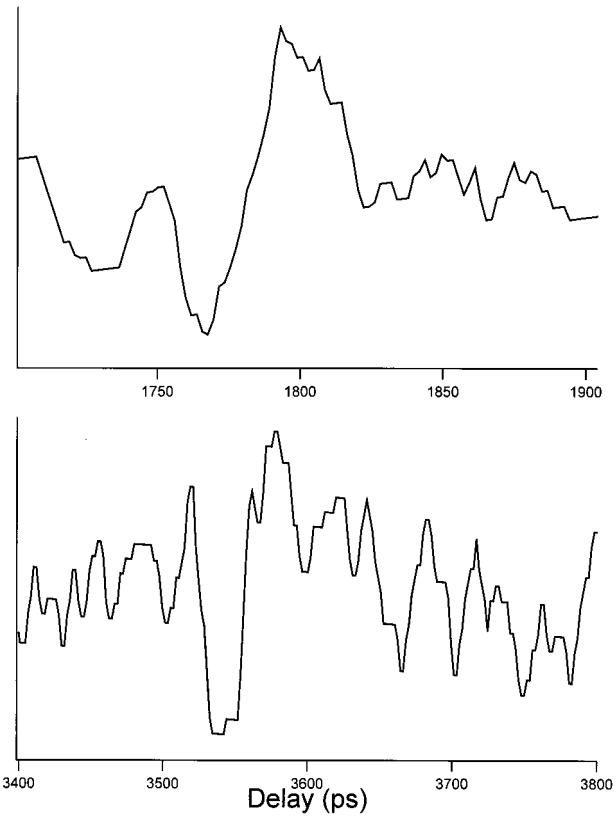

Figure 2. Expanded views of the experimental trace of Figure 1 (top) in the regions of the two RCS transients assigned as *C*-type.

Considering now what the RCS results imply about naphthalene trimer's geometry, one must choose between two possibilities, a near-prolate asymmetric top with $C = 141$ MHz, $B \simeq 193$ MHz, and a large transition-dipole projection along the *a* principal axis or an oblate (or near-oblate) species having $C = 141$ MHz, $\bar{B} = 167$ MHz, and a large transition-dipole component perpendicular to the *c* principal axis. There are two reasons to choose the latter possibility. First, there are no reasonable trimer geometries corresponding to the near-prolate case. For example, though the calculations of Gonzalez and Lim[10] yield several near-prolate species as local energy minima on ab initio and molecular mechanics IPS's, the *B* and *C* constants of such species are much too small to bear any relation to our experimental results. No such discrepancy obtains, however, for the oblate symmetric top that is the global energy minimum of these surfaces, as we discuss in more detail below.

Second, simulations of the RCS traces to be expected for the two cases also show that it is the oblate possibility that obtains. In particular, simulations for the near-prolate case show that the *J*-type transient at $1/4\bar{B}$ would be considerably smaller (relative to the one at $1/2\bar{B}$) than that observed and that the one at $3/4\bar{B}$ would be absent altogether. Further, this case would produce *C*-type transients as prominent as the largest *J*-type ones, in contrast to the observations. On the other hand, the case of an oblate symmetric top with a perpendicular transition moment gives rise to simulated traces that match the observed one closely. An example of such a simulation is shown as the middle trace in Figure 1. One notes the good agreement between experiment and simulation in almost all particulars, the one exception being the detailed shapes of the *C*-type transients. While the latter discrepancy is mildly disturbing, it can be plausibly attributed to the fact that the simulation software does not account for the effects of first-order coriolis interactions on the RCS transients. Such interactions will play a role in the spectroscopy related to the perpendicular transition of a symmetric top since such a transition must involve at least one degenerate vibronic state.[16] Moreover, the effects of such interactions on the shapes of *C*-type transients may be expected to be significant in comparison to their effects on *J*-type ones, since the former involve $|\Delta K| = 2$ coherences while the latter involve only $\Delta K = 0$ ones.[15] In contrast to the match between experimental results and Figure 1 (middle), simulations performed under the assumption of an oblate species with a parallel-type dipole do not agree with experiment, in that no *C*-type features are present for this case. This can be seen, for example, in the simulation shown in Figure 1 (bottom). In summary, then, the RCS results point to an oblate or near-oblate species having a perpendicular-type $\bar{8}_0^1$ transition moment with $\bar{B} = 167 \pm 1$ MHz and $C = 141 \pm 1$ MHz. Here, the quoted uncertainties derive from the uncertainty in the temporal positions of the transients.

To proceed further in the determination of naphthalene trimer's geometry, we invoke the conclusion from vibronic[4,7,8] and vibrational[8,9,11] spectroscopic studies that the species has three symmetrically equivalent naphthalene moieties. Such equivalence implies that the cluster must have a C_3 symmetry axis. (It is, moreover, consistent with the species being a symmetric top, as suggested by the RCS results.) The question then becomes how the equivalent naphthalene moieties are oriented with respect to the C_3 axis, a question whose answer requires, in general, the specification of four independent intermolecular coordinates. Clearly, four such geometrical parameters cannot be extracted, in general, from the two rotational constants that we have obtained via RCS. Despite this, it is possible to make a strong argument for a specific

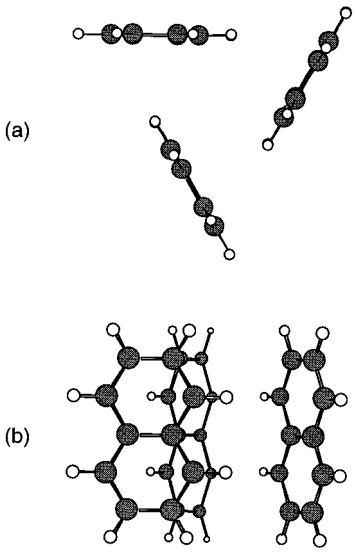

Figure 3. Two views of the minimum-energy geometry of naphthalene trimer on the intermolecular potential surface of ref 20. The view in a is down the C_3 symmetry axis (the *c* principal axis) of the species. The view in b is along an axis perpendicular to that in a.

naphthalene-trimer geometry, namely, as depicted Figure 3, one in which the long axes of the monomers are oriented parallel to or nearly parallel to the C_3 axis.

First, such a geometry is consistent with the transition dipole of the cluster's $\bar{8}_0^1$ band being perpendicular-type. The $\bar{8}_0^1$ band of naphthalene monomer is short-axis polarized.[14] Taking the transition dipole of the trimer $\bar{8}_0^1$ band to be a vector sum of monomer dipoles, one is led to the conclusion that in the trimer the monomer short axes must be perpendicular or largely perpendicular to the cluster's symmetry axis. Clearly, this is consistent with the monomer long axes being parallel to the cluster C_3 axis.

Second, the observed rotational constants are quantitatively consistent with a long-axis-parallel C_{3h} geometry. For such a geometry, the moments of inertia parallel and perpendicular to the C_3 axis are given, respectively, by

$$I_{\parallel} = 3(mR^2 + I_a)$$

and

$$I_{\perp} = 1.5(mR^2 + I_b + I_c)$$

where *m* is the mass of naphthalene monomer, *R* is the distance between any given monomer center of mass and the center of mass of the cluster, and I_a, I_b, and I_c are the *a*, *b*, and *c* moments of inertia, respectively, of naphthalene monomer. These equations represent two, independent means by which to determine *R* from the experimental data. However, they will only produce equal *R* values, in general, if the trimer actually has the long-axis parallel structure. Solving for *R* in each of these equations, given the experimentally determined values for $I_{\parallel}$ and $I_{\perp}$ along with $m = 128.06$ amu and $(I_a, I_b, I_c) = (162.76, 410.41, 571.76)$[17] amu-Å^2, gives $R = 2.84 \pm 0.01$ and 2.845 ± 0.015 Å, respectively. One has further confidence, therefore, that the long-axis-parallel geometry is the actual trimer structure.

Third, the *R* values determined above imply a monomer-to-monomer center-of-mass distance of 4.925 ± 0.020 Å in the cluster.[18] Such a value is reasonable physically. In fact, it is quite close to the 5.10-Å nearest-neighbor separation that applies to naphthalene crystal.[19]

Finally, the details of the long-axis-parallel geometry derived from the RCS data agree with calculated minimum-energy structures of naphthalene trimer. For example, the *ab initio* computed global energy-minimum geometry reported by Gonzalez and Lim[10] is of the C_{3h} long-axis-parallel type with $A = B = 166.4$ MHz and $C = 140.3$ MHz. The same structural form and similar rotational constants are obtained for the minimum-energy geometry calculated by these same authors on a molecular-mechanics potential. Yet a third example pertains to the minimum-energy geometries on semi-empirical atom−atom IPS's that are commonly employed to model aromatic−aromatic interactions. As pointed out in section I, on such potentials, too, the long-axis-parallel structure is the minimum-energy one.[8,11,12] Indeed, the trimer structure shown in Figure 3 is the minimum-energy one on the IPS taken from ref 20. The rotational constants corresponding to this computed structure ($A = B = 165$ and $C = 136$ MHz[11]) are very similar to the measured ones reported herein.

In conclusion, we have presented rotational coherence results on naphthalene trimer that, in the light of other results on the species, provide compelling evidence for a structure in which three symmetrically equivalent naphthalene moieties are oriented with their long axes parallel and are separated by 4.925 ± 0.020 Å. Given such a structure, the only intermolecular degree of freedom that remains to be determined is the tilt angle of the monomers (e.g., the angle between a given monomer's out-of-plane axis and the vector pointing from the center of mass of the cluster to that of the monomer). While the RCS results on the perprotonated trimer are not sensitive to this angle, those on mixed isotopomers should be, and RCS experiments on such species are planned. We have also provided herein the first clear demonstration that the mass-selective TRID variant of RCS can be an effective probe of the structures of relatively large molecular clusters. One expects that further application of this method will prove useful in the structural analysis of other such species.

Acknowledgment. We are grateful to the National Science Foundation (CHE 98-07372) and the Department of Energy (DE-FG03-89-ER14066) for support of this research.

References and Notes

(1) Syage, J. A.; Wessel, J. E. *J. Chem. Phys.* **1998**, *89*, 5962. Wessel, J. E.; Syage, J. A. *J. Phys. Chem.* **1990**, *94*, 737.
(2) Wessel, J. *Phys. Rev. Lett.* **1990**, *64*, 2046.
(3) Saigusa, H.; Sun, S.; Lim, E. C. *J. Phys. Chem.* **1992**, *96*, 2083.
(4) Saigusa, H.; Sun, S.; Lim, E. C. *J. Phys. Chem.* **1992**, *96* 10099.
(5) Saigusa, H.; Sun, S.; Lim, E. C. *J. Chem. Phys.* **1992**, *97*, 9072.
(6) Saigusa, H.; Lim, E. C. *Chem. Phys. Lett.* **1993**, *211*, 410.
(7) Saigusa, H.; Lim, E. C. *J. Chem. Phys.* **1995**, *103*, 8793.
(8) Schaeffer, M. W.; Kim, W.; Maxton, P. M.; Romascan, J.; Felker, P. M. *Chem. Phys. Lett.* **1995**, *242*, 632.
(9) Kim, W.; Felker, P. M. *J. Chem. Phys.* **1996**, *104*, 1147. Kim, W.; Felker, P. M. *J. Chem. Phys.* **1998**, *108*, 6763.
(10) Gonzalez, C.; Lim, E. C. *J. Phys. Chem. A* **1999**, *103*, 1437.
(11) Kim, W.; Schaeffer, M. W.; Chung, J.; Lee, S.; Felker, P. M. *J. Chem. Phys.*, submitted for publication. Schaeffer, M. W. Ph.D. Dissertation, Department of Chemistry and Biochemistry, University of California at Los Angeles, 1997.
(12) White, R. P.; Niesse, J. A.; Mayne, H. R. *J. Chem. Phys.* **1998**, *108*, 2208.
(13) Ohline, S. M.; Romascan, J.; Felker, P. M. *Chem. Phys. Lett.* **1993**, *207*, 563.
(14) For example, see: Stockburger, M.; Gattermann, H.; Klussman, W. *J. Chem. Phys.* **1975**, *63*, 4519. Beck, S. M.; Powers, D. E.; Hopkins, J. B.; Smalley, R. E. *J. Chem. Phys.* **1980**, *73*, 2019.
(15) For example, see: Felker, P. M. *J. Phys. Chem.* **1992**, *96*, 7844. Joireman, P. W.; Connell, L. L.; Ohline, S. M.; Felker, P. M. *J. Chem. Phys.* **1992**, *96*, 4118.
(16) For example, see: Herzberg, G. *Electronic Spectra of Polyatomic Molecules*; Van Nostrand Reinhold: New York, 1996; pp 224, 230−237.

(17) Majewski, W.; Meerts, M. L. *J. Mol. Spectrosc.* **1984**, *104*, 271.
(18) It is worth noting that the particular values of *R* and the naphthalene−naphthalene separation in the trimer, as derived from the measured rotational constants, are dependent on the naphthalene monomer geometries. Presumably, this is the reason that the naphthalene−naphthalene separation quoted herein is slightly different than that quoted in ref 10, despite agreement between the trimer's rotational constants in the two works.
(19) For example, see: Hanson, D. M. *J. Chem. Phys.* **1970**, *52*, 3409.
(20) Williams, D. E.; Xiao, Y. *Acta Crystallogr. A* **1993**, *49*, 1.